https://doi.org/10.5194/se-2019-187
Preprint. Discussion started: 13 December 2019

Solid Earth Discussions

Oligocene-Miocene extension led to mantle exhumation in the central Ligurian Basin, Western Alpine Domain

Anke Dannowski[1], Heidrun Kopp[1,2], Ingo Grevemeyer[1], Dietrich Lange[1], Martin Thorwart[2], Jörg Bialas[1], and Martin Wollatz-Vogt[1]

[1]GEOMAR Helmholtz Centre for Ocean Research Kiel, Germany
[2]CAU, Christian-Albrechts-Universität zu Kiel, Germany

Correspondence to: Anke Dannowski (adannowski@geomar.de)

Abstract. The Ligurian Basin is located in the Mediterranean Sea to the north-west of Corsica at the transition from the western Alpine orogen to the Apennine system and was generated by the south-eastward trench retreat of the Apennines-Calabrian subduction zone. Late Oligocene to Miocene rifting caused continental extension and subsidence, leading to the opening of the basin. Yet, it still remains enigmatic if rifting caused continental break-up and seafloor spreading. To reveal its lithospheric architecture, we acquired a state of the art seismic refraction and wide-angle reflection profile in the Ligurian Basin. The seismic line was recorded in the framework of SPP2017 4D-MB, the German component of the European AlpArray initiative, and trends in a NE-SW direction at the centre of the Ligurian Basin, roughly parallel to the French coastline.

The seismic data recorded on the newly developed GEOLOG recorder, designed at GEOMAR, are dominated by sedimentary refractions and show mantle Pn arrivals at offsets of up to 70 km and a very prominent wide-angle Moho reflection. The main features share several characteristics (i.e. offset range, continuity) generally associated with continental settings rather than documenting oceanic crust emplaced by seafloor spreading. Seismic tomography results are augmented by gravity data and yield a 7.5-8 km thick sedimentary cover which is directly underlain by serpentinised mantle material at the south-western end of the profile. The acoustic basement at the north-eastern termination is interpreted to be continental crust, thickening towards the NE.

Our study reveals that the oceanic domain does not extend as far north as previously assumed and that extension led to extreme continental thinning and exhumation of sub-continental mantle which eventually became serpentinised.

1 Introduction

The Ligurian Sea is situated in the north-western Mediterranean Sea at the transition from the western Alpine orogen to the Apennine system. The geodynamical setting of the area is controlled by the convergence of the African and Eurasian plates (e.g. Dercourt et al., 1986). Despite the existing large collection of seismic and other geophysical data, the present-day crustal architecture of the Ligurian Basin is still under discussion and the kinematic boundaries are poorly resolved, in particular, the continent-ocean transition (COT) along the margins as well as its termination to the north-northeast. Imaging clear fault structures within the crust has proved challenging due to the presence of thick Messinian salt layers and due to the time of

https://doi.org/10.5194/se-2019-187
Preprint. Discussion started: 13 December 2019

arrival of the first seafloor multiple which roughly coincides with the arrival of the reflection of the acoustic basement (Béthoux et al., 2008). Deep drilling data are lacking and the magnetic data are complex and anomalies discontinuous (Bayer et al., 1973). Based on integrated seismic and magnetic data, maps indicating the extent of the oceanic domain were created (i.e. Burrus, 1984; Gueguen et al., 1998; Rollet et al., 2002), however, no axial ridge was imaged near the centre of the basin (Rollet et al., 2002). The crust in the north-eastern basin was interpreted to be atypical oceanic crust (Mauffret et al., 1995; Chamot-Rooke et al., 1997; Contrucci et al., 2001; Rollet et al., 2002) to explain the mismatch between the expected oceanic domain and the observed seismic signal. A clear change from continental to oceanic crust was only shown for the southern area of the Ligurian Basin, in the Gulf of Lion and offshore Sardinia (Gailler et al., 2009). It is proposed that the oceanic domain is separated from the continental margins by a transitional domain characterised by a high-velocity lower crust (Fig. 1). A good overview of seismic experiments until 2002 is presented in Rollet et al. (2002). Furthermore, the area was revisited or data were re-analysed with modern seismic techniques including the CROP deep seismic profiles (Finetti et al., 2005), the TGS-NOPEC and the SARDINIA profiles (Gailler et al., 2009; Jolivet et al., 2015), as well as more recent studies along the French and Italian Riviera with the 3D seismic refraction GROSMarin project (Dessa et al., 2011) and an amphibious ambient noise study (Guerin et al., 2019).

In the frame of the LOBSTER project, we add a new state-of-the-art seismic refraction line to the database (Fig. 1, red line with orange and yellow triangles). Here, we present the analysis of the seismic refraction line in the central Ligurian Basin, which is the extension of a pre-existing profile (Makris et al., 1999), which we call MAKRIS (Fig. 1, black line). We aim to unravel the present-day crustal structure and its nature in the centre of the Ligurian Basin, map the depth of the crust-mantle boundary (seismic Moho), and reveal the styles of deformation during the last extensional phase. We investigate the hypothesis that the Oligocene-Miocene extension led to either hyper-extended continental crust or serpentinised sub-continental mantle below post-rift sediments in the north-eastern Ligurian Basin. A further objective is to provide a seismic velocity model as a contribution to an improved seismic event localisation in the offshore region.

2 Geological structures and geodynamics of the Ligurian Sea and the Corsica-Sardinia block

The Ligurian Sea has a width of ~150 km from the northern tip of Corsica to the Ligurian coast near the city of Sanremo. It widens towards the southwest to ~175 km between Calvi (Corsica) and Cannes. South of the imaginary line between Ajaccio (Corsica) and Toulon, the basin is roughly 225 km wide. The basin opens entirely towards the Balearic Sea. The Ligurian Basin itself is smaller with a width of 70 km, 120 km, and 170 km, respectively, along the three dashed grey lines in Figure 1 and the seafloor reaches depths of ~2700 m. The Ligurian margin is characterised by a narrow and steep slope (10-20 km) with a few listric normal faults (Finetti et al., 2005). The Corsica slope is wider (20-50 km) and the margin is characterised by several listric faults extending over a wider area (Dessa et al., 2011).

The Ligurian Sea formed as a back-arc basin at the transition from the western Alpine orogen to the Apennine system (e.g. Doglioni et al., 1997; Faccenna et al., 1997; Rehault et al., 1984). The Alpine transition is characterised by a change in

https://doi.org/10.5194/se-2019-187
Preprint. Discussion started: 13 December 2019

subduction polarity between the two orogens (Jolivet and Faccenna, 2000; Handy et al., 2010). The Ligurian Basin is the oldest back-arc basin in the Western Mediterranean Sea and developed from Late Oligocene to Early Miocene (Réhault and Béthoux, 1984; Roca and Desegaulx, 1992; Fernàndez et al., 1995; Jolivet and Faccenna, 2000; Rosenbaum et al., 2002; Finetti et al., 2005; Advokaat et al., 2014). The extension is related to the south-east trench retreat of the Apennines-Calabrian subduction zone initiated in the Oligocene (Montigny et al., 1981; Réhault and Béthoux, 1984; Vigliotti and Langenheim, 1995; Gueguen et al., 1998; Rosenbaum et al., 2002; Faccenna et al., 2001).

Rifting has initiated ~30 Ma ago at a rate of ~1 cm/yr in the NE and ~2 cm/yr in the SW (Rollet et al., 2002). The initiation is associated with magmatism on land along the western Ligurian margin (Rollet et al., 2002). At roughly 21 Ma, rifting terminated while an anticlockwise rotation of the Corsica-Sardinia block was initiated (Rollet et al., 2002; Speranza et al., 2002). During this phase, the commencement of oceanic spreading was proposed (Pascal et al., 1993; Contrucci et al., 2001; Rollet et al., 2002; Finetti et al., 2005). These authors referred to tholeiitic volcanic edifices to solidify their interpretation and interpreted the pattern of magnetic data (Bayer et al., 1973) to be a result of two main discontinuous volcanic lineaments, sub-parallel to the basin axis related to oceanic spreading and unroofing of mantle material. The opening of the Ligurian Basin ended ~16-15 Ma ago and was associated with a second calc-alkaline volcanic phase along the Corsican margin (Rollet et al., 2002) that is linked to the migration of the subducting lithosphere towards the E-SE. The extension of the Ligurian Basin stopped and shifted to the Tyrrhenian Sea while the Apennines-Calabrian subduction zone continued to roll back further southeast until late the Messinian, ~6 Ma (Faccenna et al., 2001; Advokaat et al., 2014). The opening rate was calculated with 7.8-10.3 mm/yr (Moeller et al., 2013). In the north, extension led to continental crustal thinning (Moeller et al., 2013), while further south in the centre of the Tyrrhenian Basin, mantle was exhumed and serpentinised and intruded by Mid-Ocean-Ridge type (MOR-type and intraplate basalts) (Prada et al., 2016). Similar to the Ligurian Basin, the Tyrrhenian Sea shows distributed, non-linear magnetic anomalies (Cella et al., 2008). Anomalies often coincide with volcanic islands, seamounts or other morphological units of igneous composition. During the Ocean Drilling Project (ODP) Leg 107 at site 651, serpentinised mantle rocks were drilled forming the top of the basement (Bonatti et al., 1990).

Gueguen et al. (1998) and Rollet at al. (2002) suggest that the central Ligurian Basin is comprised of oceanic crust. The authors divided the basin into different zones of continental and oceanic domains based on seismic, magnetic and gravity data (Fig. 1): (1) atypical oceanic crust with (2) transitional zones to (3) continental crust. The location of the northeast-southwest trending continent-ocean transition is proposed to be situated in the vicinity of the volcanic Tristanites Massif (Fig. 1) (Makris et al., 1999) (yellow line perpendicular to the MAKRIS profile in Figure 1). Based on re-analysed expanding spread profiles (ESP), Contrucci et al. (2001) proposed a 40 km wide area of oceanic crust near the Median Seamount (Fig. 1).

https://doi.org/10.5194/se-2019-187
Preprint. Discussion started: 13 December 2019

3 Data acquisition, processing, and modelling

Data at different scales resolving the subsurface structure were acquired in the Ligurian Sea in February of 2018 during the cruise MSM71 aboard the German research vessel Maria S. Merian (Kopp et al., 2018). Active seismic refraction data were obtained along the centre of the basin. Our NE-SW trending seismic refraction and wide-angle reflection line is situated in the prolongation of an existing refraction profile in the northern Ligurian Basin (Makris et al., 1999) (Fig. 1) and is presented here.

3.1 Data acquisition and processing

The active seismic data were simultaneously recorded on short period ocean bottom seismometers (OBS) and ocean bottom hydrophones (OBH) as well as on a short streamer (280 m long) that was towed behind the vessel in 5 m water depth. Additionally, Parasound data were recorded along the profiles. The 127.5 km long refraction seismic profile consists of 15 OBH/OBS at a station spacing of ~ 8km (Fig. 1). A total of 1079 shots were fired by an 84-liter G-gun array at an interval of 60 s, resulting in a shot interval of ~123 m. The location of the stations on the seafloor was estimated using the symmetry of the direct water arrivals from the shots on both sides. The airgun shots were recorded using newly developed GEOLOG loggers, designed at GEOMAR. All recorders ran reliable during the deployment of 2 days with a negligible absolute clock drift between -1.03 ms to +0.72 ms. The sampling frequency is 250 Hz. The data processing included the conversion of the continuous data from GEOLOG format into standard continuous SEG-Y format using the GEOLOG programming interface. Afterwards, the continuous SEG-Y data were converted into standard trace-based SEG-Y format (Fig. 2b). Simultaneously, the clock drift was corrected, a step important for OBS data, since the instruments cannot be continuously synchronized via GPS during deployment as commonly done onshore. A gated Wiener multi-trace deconvolution with an autocorrelation average of 51 traces was applied to the shot gathers to compress the basic wavelet, to leave the Earth's reflectivity in the seismic trace and to remove the source signature and the hydrophone and geophone responses.

3.2 The GEOLOG recorder

The GEOLOG is a 32-bit seismic data logger designed to digitise data from a three-component seismometer and a hydrophone. We recorded the hydrophone output on two channels (channels 1 and 5) at two different amplification levels providing well amplified long-range records (gain=16) and preventing clipped amplitudes from short-range airgun shots (gain=1) to minimise difficulties with amplitude restoration because no gain range was implemented. The gain for the three seismometer channels 2 to 4 was set to 16. Two additional analogue pins can be used as general-purpose input/output (GPIO) for measuring power levels for example. 3.3 V and 5 V connectors can serve external devices. Sampling intervals between 50 Hz and 4 kHz are controlled either by an atomic clock or a temperature compensated clock (SEASCAN). We used an external GPS receiver for synchronization of the internal clock prior and after deployment, which was driven by the GEOLOG itself. Our seismic data were stored on two micro SD cards with a volume of 32 GB each. The recorder has been tested and proved reliable for writing speeds and SD cards of up to 128 GB (larger capacities are possible). The low power consumption of 375 mW (average battery

https://doi.org/10.5194/se-2019-187
Preprint. Discussion started: 13 December 2019

drain) allowed us to save batteries. We used only 8 alkaline batteries per station for our short-term deployment. Thus, using lithium batteries, long-term deployments of more than 9 months can be performed. Battery power can further be saved by a delayed start of recording up to 31 days after programming. We set the recording parameters, i.e. the number of channels, gain and sampling rate, using the graphical user interface. The recorders can be programmed through any terminal program on a Windows or Linux operating system. The programming device was connected via RS232 using an RS232-USB adapter. A second RS232 interface can be used to drive external sensors (e.g. levelling of broadband seismometers). The GPS system used for the internal clock time synchronisation was developed together with the recorder and can operate with GPS, GLONASS, GALLILEO and QZSS enabling operation worldwide and in polar regions. Besides stable output of NMEA and PPS, the German DCF-77 code is also available. Moreover, the GPS system is available to deliver time or distance based trigger with TTL output, NMEA sequence and records of time stamps on an SD card.

3.3 Data description and analysis

The airgun shots can be followed for offsets up to 60 km on all 15 stations (Fig. 2). In general, the sections look very similar with clear sedimentary arrivals and wide-angle Moho reflections (PmP) as well as mantle phases (Pn) at a critical distance between 25 km and 35 km to the stations (Fig. 2a). Although phase arrivals show common features in all record sections (Fig. 2a), the characteristics of the seismic phases change slightly from south to north (Fig. 2b-2d).

As a result of decreasing water depth towards the northeast, the direct waves through water (Pw) arrive later at the southern stations than at the northern stations (Fig. 2a). The picks from a shallow sedimentary reflection phase (PsP) arrive approximately 0.5 s to 1 s after the direct arrival and result from the top of salts that become shallower towards the north (as imaged in the multichannel seismic data in Fig. 3a). The red picks (Ps1) and the orange picks (Ps2) (Fig. 2b-2d) are interpreted as refracted phases through Plio-Quaternary and older sediments, respectively. The apparent seismic velocity of the Ps2 is very constant at ~4.3 km/s to ~4.6 km/s. The phase shows many undulations and some shadow zones caused by the salt unit that displays intense doming and is possibly disrupted by some volcanic structures that are imaged in the MCS and the Parasound data (Fig. 3). This phase continues as a secondary arrival (Ps3) with a similar apparent velocity of ~4.6 km/s at the southern stations but disappears at the northern stations. Based on the apparent velocity and forward modelling, we interpret phase Ps3 as a refracted phase through the sediments. Simultaneously, when phase Ps3 disappears (from OBS208 towards the north), an additional refracted phase (Pg) (green picks in Fig. 2c-2d) occurs and becomes longer northwards. The phase has an apparent velocity of ~6.2 km/s. At an offset of about 25 km, an abrupt change in the apparent seismic velocity for the first arrival occurs to apparent velocities of ~8 km/s, as typically observed in the oceanic upper mantle. The yellow picks (Fig. 2b-2d) are refracted mantle phases (Pn) at the northern stations and show a similar apparent seismic velocity of ~8 km/s. However, the critical distance moves to slightly larger offsets at about 30 km. Furthermore, an earlier very short reflection occurs at 20-25 km offset. The gravimetric data (Fig. 5a) show a change approx. 20 km south of OBS208. Pn phases at the southern stations are very weak, while the PmP is relatively strong compared to typical oceanic crust characteristics.

https://doi.org/10.5194/se-2019-187
Preprint. Discussion started: 13 December 2019

3.4 P-wave traveltime tomography modelling strategy and parameters

A preliminary seismic velocity model was build using RAYINVR (Zelt, 1999) to (1) reveal the overall structure of the data, (2) manually assign the picked phases to certain layers, and (3) serve as starting model for the travel time tomography. Travel times were picked on the hydrophone channels using the interactive analysis tool for wide-angle seismic data PASTEUP (Fujie et al., 2008). The vertical seismometer component was used for picking to confirm and to complement the picks observed on the hydrophone channel. Multiples were picked in addition and used during the forward modelling approach to confirm the layer boundaries and seismic velocities. Thereafter, a travel time tomographic inversion (tomo2D from Korenaga et al. (2000)) was applied to invert the seismic P-wave velocity model and yield model uncertainties. In a first step only near offset picks with distances smaller than 15 km were inverted. Subsequently, all first arrivals and the mantle reflections were inverted with a set of starting models that converged to chi² values of less than 1 within 5 iterations. To test the model space and its limits, the starting models were manually created using rayinvr (Zelt, 1999). To carefully evaluate the resulting velocity models we used three criteria: (1) travel times need to fit the data (Fig. 2a), (2) travel time residuals, RMS misfit and chi² had to be low (i.e. chi2 ~ 1), and (3) the gravity response (calculated after a velocity-density conversion) (Korenaga et al., 2001) of the resulting density model must yield comparable results to the satellite gravity data. Based on the evaluation, 17 models were chosen to generate an average model for the crustal part (Fig. 4a, above the Moho) and the standard deviation was calculated (Fig. 4b). Overall, the standard deviation in the crust down to the acoustic basement is smaller than 0.15 s, indicating small differences between the inverted velocity models and hence an excellent resolution. In a further step, the average model was edited by adding different 1D profiles with mantle velocities underneath the crust-mantle boundary. A set of 12 mantle velocity starting models was used to invert for refracted mantle phases. Again, an average model and the standard deviation for the mantle were calculated (Fig. 4c). Standard deviations for the mantle P-wave velocities are small (<0.1 s), indicating a good resolution of upper mantle velocities. Lastly, the very short reflected phases interpreted to result from the top of continental crust were calculated as a floating reflector without implementing a velocity discontinuity into the model to confirm the top of crust, i.e. the crystalline basement.

4 Results

4.1 Seismic P-wave velocity distribution

In general, the average P-wave velocity along the profile (Fig. 4a) shows only minor lateral variations, mainly caused by the salt layers and the corresponding tectonic features at 4-6 km depth. The uppermost portion of the velocity model is characterised by a strong velocity gradient of ~1 s^{-1} that is laterally very constant. P-wave velocities increase from 2.2 km/s at the seafloor to 3.5 km/s approx. 1.3 km below the seafloor. We interpret this unit as Plio-Quaternary sediments mixed with the upper evaporite unit after Rollet et al. (2002), using their multi-channel seismic data profile MA24 (Fig. 1, inlay profile 6). The Plio-Quaternary sediments are imaged as horizontally layered strata in the multi-channel seismic data in Figure 3a. This

https://doi.org/10.5194/se-2019-187
Preprint. Discussion started: 13 December 2019

high velocity-gradient layer thins towards the north, from 1.5 km to 1.2 km thickness, respectively, and shows slightly slower velocities at the southern end (2.2 km/s) compared to the northern end (2.4 km/s) at the seafloor. Between ~4 km and 6 km depth, the velocities range from 3.5 km/s to 4.5 km/s, and there are areas where minor velocity inversions are observed. These low velocity units have a lateral extent of up to 10 km and a velocity contrast of up to ~0.2 km/s. We identify this section as the Messinian salt unit. From 6 km to ~10 km depth, the seismic velocities increase from ~4.5 km/s at the top to 5.7 km/s at the bottom. We interpret this section as Pre-Messinian down to syn-rift sediments, possibly from Aquitanian related to Jolivet et al. (2015).

The acoustic basement occurs at a depth from 10 km to 11.5 km below the sea surface. In the north-eastern half of the profile, starting roughly at profile KM 70 (Fig. 4a), the basement velocities increase from 5.8 km/s to 6.6 km/s; they are interpreted, based on absolute velocities, as continental crust, thickening towards the north. The acoustic basement here is at a depth of ~10 km below the sea surface. At the opposite southern half of the profile, a strong velocity jump occurs from 5.7 km/s to ≥7.3 km/s. We interpret this part of the acoustic basement as the crust-mantle boundary (Moho). The uppermost mantle is characterised by seismic velocities >7.3 km/s that increase to ~8 km/s over a depth interval of 2-3 km. The histogram (Fig. 5b) images a gap in seismic velocities between 6.6 km/s and 7.3 km/s, which suggests that no fresh oceanic crust material (gabbroic rocks) is present along the profile.

4.2 Gravity modelling

To constrain the crustal structure along the profile, we calculated the gravity response (Talwani et al., 1959) of the final seismic velocity model and compared it to the free-air gravity anomaly derived from satellite data (Sandwell et al., 2014). The fact that the profile is situated in the centre of the basin allows us to assume that only minor 3D side-effects occur in our 2D-modelling approach, caused by topography. The velocity-depth distribution was used to assign densities by applying different density-velocity relations. The water layer is assumed to have a density of 1.03 g/cm³. Gardeners rule, $\rho = 1.74 * Vp^{0.25}$, valid for sediments between 1.5 km/s < Vp < 6.1 km/s (Gardner et al., 1974), was used for the sedimentary layers. For crystalline (non-volcanic) rocks: $\rho = 0.541 + 0.3601 * Vp$ (Christensen and Mooney, 1995) was used. A density of 3.3 g/cm³ was assigned for the mantle. In areas with reduced seismic mantle velocities, the mantle density was reduced to 3.15 g/cm³ (Carlson and Miller, 2003). The converted densities explain the observed free-air gravity anomaly for the part covered by our deployed instruments. We extended the profile further northeast with the marine part of the MAKRIS line (Fig. 1, inlay profile 4). From profile KM 127.5 northwards, we related the gross density model structure to the results of the MAKRIS line (Makris et al., 1999). However, we removed a large step of 10 km in Moho depth and replaced it by a more gradually deepening Moho, which follows closely the top of the layer of underplating in the MAKRIS line. The fit of observed and calculated gravity data is reasonably well supporting the interpretation of a thickening continental crust towards the northeast.

https://doi.org/10.5194/se-2019-187
Preprint. Discussion started: 13 December 2019

5 Introduction Section (as Heading 1)

5.1 Nature of the lithosphere

The seismic velocity model along our refraction profile (Fig. 4a) shows no common features for oceanic crust. Oceanic crust typically consists of a high-velocity gradient in Layer 2 and a lower velocity gradient in Layer 3 (e.g. White et al., 1992; Grevemeyer et al., 2018; Christeson et al., 2019). The absolute seismic velocities are highly variable, however, for a gabbroic crust, velocities are typically between 6.7 km/s and 7.2 km/s (Grevemeyer et al., 2018; Christeson et al., 2019). The histogram in Figure 5e shows a gap for this range of velocities suggesting that no typical oceanic crust and no thick layer of gabbroic rocks are present along the profile. In any case, the lack of seismic velocities expected for oceanic crust does not support the occurrence of larger units of oceanic crust as observed in the Tyrrhenian Sea (Prada et al., 2014).

Continental crust is characterised by a low seismic velocity gradient throughout the crystalline crustal layers and shows typical velocities of ~5.8 to ~6.6 km/s (Christensen and Mooney, 1995). We observe this velocity range in the northern half of the profile, starting from profile KM70, at a depth of 10 km to 13 km. The observed seismic velocities only leave two possible interpretations: (1) hyper-extended continental crust or (2) a laterally isolated magmatic intrusion within the sedimentary units feeding the volcanic extrusion observed in the MCS and Parasound data (Fig. 3). Based on the gravity model (Fig. 5), we favour the first scenario of extremely thinned continental crust, pinching out towards the SW, leading to exhumed mantle during the rifting phase in the southern half of the profile. Based on the velocity model (Fig. 4a) it is not possible to distinguish whether the crystalline basement there is upper, middle, or lower continental crust. A continental crustal thickening towards the north-east is as well supported by the modelling of the free air anomaly (Fig. 5). Additionally, a thickening crustal layer supports the interpretation as continental crust, since we would expect the COT to be manifested in an abrupt change from oceanic to continental crust or to gradually thin out towards the NE, towards the rotational pole (Rosenbaum et al., 2002), depending on the situation of the profile with respect to the proposed spreading axis.

An expanding spread profile (ESP) (Le Douaran et al., 1984; Contrucci et al., 2001) crosses the northern end of our profile (Fig. 1, inlay profile 5). There the crust-mantle boundary was defined at a depth of 13-15 km while the acoustic basement was observed at ~9 km depth. Contrucci et al. (2001) retrieved crustal velocities of 6.3 - 6.9 km/s for the basin centre, which in general, is in good agreement with our results. Based on MCS data (LISA01) (Contrucci et al., 2001) with an observed major step in the basement on the Ligurian margin, they interpreted the central basin as an oceanic domain. On the Corsica margin, this major step was not observed, however, magnetic anomalies were used to constrain the interpretation. The MCS data resolve only the sedimentary portion of the crust and give no information on the internal structures of the crystalline basement itself, thus, a different explanation for the major step in the basement near the Ligurian margin could be that upper-crustal blocks sit on top of continental mantle similar to the Galicia margin (Nagel and Buck, 2004). Our profile only provides information on the basin centre where the absolute velocities of Le Douaran et al. (1984) and Contrucci et al. (2001) fit continental crust velocities very well and support our interpretation of mantle material beneath thinned continental crust observations.

https://doi.org/10.5194/se-2019-187
Preprint. Discussion started: 13 December 2019

The velocity model for the southern half along our refraction profile is well constrained (Fig. 5b). Seismic velocities of ~7.3 km/s and higher are too fast for magmatic crust (Grevemeyer et al., 2018; Christeson et al., 2019). Seismic velocities of unaltered mantle are >7.8 km/s (Carlson and Miller, 2003; Grevemeyer et al., 2018). Based on the seismic P-wave velocities, we interpret the uppermost mantle to be serpentinised, which is supported by the Pn phases that are weak in amplitude at the southern stations (Fig. 2). P-wave velocities of ~7.5 km/s in the south-western half of the profile (Fig. 4a) are in-line with ~20% serpentinisation (Carlson and Miller, 2003). From OBS204 to OBS207, the PmP phase is extremely high in amplitude and unusually clearly visible over a wide distance of up to 20 km (in ~10 km to ~30 km offset to the station). This area (profile KM40-KM60) is marked by Vp > 7.8 km/s directly underneath the basement, possibly an area of unaltered mantle or a result of a mafic intrusion. The fact that the mantle is partly serpentinised implies that syn-rift sediments (nowadays showing high P-wave velocities) were directly deposited on top of the mantle or brittle continental crust (Pérez-Gussinyé, 2013). Thus, structurally, the Ligurian Sea is mimicking the Atlantic non-volcanic passive margins of Iberia (Minshull et al., 2014) and Goban Spur (Bullock and Minshull, 2005).

Stretching of the crust as a result of the opening of the basin becomes less intense towards the north and thus controls the NE termination of the ultra-thin continental crust. Further south, no crystalline crust, neither of continental type nor of oceanic type is observed until the SW end of the profile. This is supported by the magnetic data (Bayer et al., 1973), which does not show the typical oceanic crust pattern of magnetisation stripes, but rather a lateral patchy pattern of magmatic domains. Further, the extension of the basin decreases towards the north, assuming oceanic crust to be present the crust should become less evolved towards the proposed ridge axis tip. However, our seismic data and gravity data indicate a gradual thickening of the crystalline crust, at least a gradual deepening of the mantle.

5.2 Continent-ocean transition

The MCS line MA24 (Rollet et al., 2002) was shot along an ESP profile consisting of four stations with a spacing of ~35 km (Le Douaran et al., 1984). The two transects are crossing our profile at the southern end (Fig. 1, inlay profile 6). The MCS data resolve sedimentary units, while the seismic velocities retrieved along the ESP profile show no absolute seismic velocities similar to oceanic crust. Both transects do not map a spreading axis. Further west along the Ligurian margin, a multichannel seismic study (Jolivet et al., 2015) and a wide-angle refraction seismic study (Gailler et al., 2009) of the Ligurian margin (Fig. 1, inlay profiles 2a and 3), in the Gulf of Lion, show a wide continent-ocean transition zone. The travel time tomography model along the OBS profiles (Gailler et al., 2009) images a succession of three domains: (1) continental, (2) transitional, and (3) oceanic domain towards the basin centre, following the zonation of Rollet et al. (2002). The same succession was found for both continental margins, however, the Corsica margin's transitional zone is much narrower. The transitional domain is interpreted to consist of a mixture of continental crust, exhumed mantle, and magmatic intrusions (Gailler et al., 2009; Rollet et al., 2002). In contrast, Jolivet et al. (2015) interpret the transitional zone as exhumed lower continental crust overlying the continental mantle which is in the distal part exhumed and serpentinised. The exhumation of lower continental crust in the Gulf of Lions is still debated. For example, numerical modelling of continental rifting at the magma-poor Galicia margin

https://doi.org/10.5194/se-2019-187
Preprint. Discussion started: 13 December 2019

showed that the lower crust is scarcely preserved or absent in the continental tip (Nagel and Buck, 2004). Our velocity model at the base of the continental crust is not well enough resolved (Fig. 4b) to distinguish between upper and lower continental crust, but we emphasize again, that we can exclude oceanic crust based on the seismic velocity distribution (Fig. 4e) and the results of gravity modelling (Fig. 5) along our seismic profile. The oceanic domain on both conjugated margins in the Gulf of Lion (Fig. 1, inlay profile 2a) and offshore Sardinia (Fig. 1, inlay profile 2b) was imaged in the travel time tomographic approach with the typical pattern observed at mid-ocean ridges (Gailler et al., 2009), with a high velocity gradient in the upper oceanic crust and a low velocity gradient in the lower crust.

5.3 Mantle exhumation and magmatic intrusions

The extension process in the Ligurian Basin stopped roughly 16 Ma and was replaced by the extension and opening of the Tyrrhenian Sea as the Apennines-Calabrian subduction zone continued to roll back. The magnetic data (Bayer et al., 1973; Cella et al., 2008) in both basins show a similar anomaly distribution with discontinuous, partially isolated anomalies. Prada et al. (2014) analysed a seismic refraction profile crossing the Tyrrhenian Sea from Sardinia to Italy mainland. Similar to the Ligurian Basin, the western margin is more elongated than the eastern margin. The authors divide the analysed profile into 3 different domains from Sardinia to the central basin: In domain #1 continental crust thins from 22 km to 13 km over a distance of 80 km. Domain #2 is interpreted as magmatic back-arc crust with blocks of continental crust. The change from continental to magmatic crust is marked by an abrupt increase of seismic velocities to >7 km/s in the lower crust, similar to the observation of Gailler et al. (2009) on the Ligurian Basin side of Sardinia. Prada et al. (2014) interpret the seismic velocities, which are slightly lower than found in 0-7 Ma old-oceanic crust, to be a result of back-arc spreading close to the active volcanic arc. Domain #3 is interpreted to be composed of serpentinised mantle to a depth of 5-6 km with basaltic intrusions. The authors summarise that rifting in the Central Tyrrhenian Basin started with extension of continental crust, continued with back-arc spreading, followed by nearby mantle exhumation. Later, the area underwent magmatic episodes with magmatic intrusions into the sedimentary layer or cropping out, forming volcanoes. These volcanoes and magmatic intrusions could be related to magnetic anomalies (Prada et al., 2016). Using the Tyrrhenian Sea as an analogy, we suggest that many of the isolated magnetic anomalies in the Ligurian Sea are caused by magmatic intrusions or extrusions manifested as volcanic edifices (Median Seamount, Tristanites Massif, Monte Doria; see Fig. 1) (Rollet et al., 2002), rather than related to a spreading axis, which was indeed not mapped in MCS data so far. However, in MCS data, intrusions of volcanic sills into younger sediments were observed (Finetti et al., 2005). At the Monte Doria Seamount 11-12 Ma old basalts were sampled by dredges and submersible dives (Rollet et al., 2002; Réhault et al., 2012), clearly indicating post-rift magmatism. Further, volcanism related to the slab roll-back of the Apennines-Calabrian subduction zone was observed at the Ligurian continental margin and dated to the initiation of the rifting phase (Rollet et al., 2002). Volcanism was as well associated with the end of the opening of the Ligurian Basin and related to the trench retreat of the Apennines-Calabrian subduction zone (Rollet et al., 2002). This implies that volcanism also occurred during the rifting phase and could add to the discontinuous magnetic anomalies.

https://doi.org/10.5194/se-2019-187
Preprint. Discussion started: 13 December 2019

5.4 Opening of the Ligurian Basin

Two different conceptual scenarios of rifting could explain our observations: (1) Rifting causing continental crust to thin until continental lower crust and mantle are exhumed and afterwards oceanic spreading is induced as observed in the Gulf of Lion (Gailler et al., 2009; Jolivet et al., 2015). (2) Rifting causing continental crust to thin until back-arc spreading is initiated and the continuation of extension leads to exhumation of mantle with magmatic intrusions (Prada et al., 2016).

Depending on the scenario, our profile is situated in the Ligurian transitional domain #2 or in the Tyrrhenian domain #3. Rifting scenario (2) would imply that well developed oceanic back-arc crust should occur southeast and northwest of the profile. The transect reaches into the area of a 3D seismic study of the Ligurian margin offshore Sanremo (Dessa et al., 2011). The authors state that they were surprised not to see a distinct change in the velocity field at the COT. Dessa et al. (2011) could not show clear evidence for a kind of back-arc crust as shown by Prada et al. (2014) or Gailler et al. (2009). However, continental crustal thinning is well imaged. Considering these aspects, we rather favour rifting scenario (1) which is also supported by the conceptual model described by Decarlis et al. (2017) for the evolution of magma-poor rifted margins. The model includes three phases of extension: (1) An initial stretching phase forming widely distributed half-grabens in the upper crust. Afterwards (2) a thinning phase leads to hyper-extended crust and is followed by (3) an exhumation phase during which subcontinental mantle rocks were exhumed.

Furthermore, the Ligurian Basin width in our study area (70 - 120 km) is much narrower than further south (~200 km) where domain #2 is summing up to ~100 km in length for both conjugated margins together. This would fill the basin in our study area, leaving little or no space for oceanic spreading. This is i.e. supported by petrological and geophysical observations at the West Iberia margin, that suggest that a COT zone can reach a width of up to 200 km (Pérez-Gussinyé, 2013).

Additionally, the opening rate becomes slower towards the north and the grade of stretching becomes less, due to the anti-clockwise rotation of the Corsica-Sardinia block. A crustal thickening towards the north would be in good agreement with the anti-clockwise rotation of the Corsica-Sardinia block and an associated gradual opening of the Ligurian Basin. This could imply that oceanic spreading was not initiated during the Oligocene-Miocene extension in the northern Ligurian Basin, along the southern half of our line. Continuing further north, extension lead to extreme thinning of continental crust, but lasted not long enough to exhume mantle.

6 Conclusion

The P-wave velocity model determined in this study images the uppermost lithospheric structure of the north-eastern central Ligurian Basin. Syn- and post-rift sediments of 7.5-8 km thickness filled the basin during and after the 15 Ma long lasting opening phase. The southern half of the profile shows contact between sediments and serpentinised mantle, while the northern half of the profile indicates a northward thickening of continental crust and a deepening crust-mantle boundary from 11 km to 13 km. Based on the retrieved velocity distribution, gravity modelling and results of surrounding studies, we conclude that the extension of the Ligurian Basin led to (1) hyper-extended continental crust and exhumed serpentinised mantle and (2) a

https://doi.org/10.5194/se-2019-187
Preprint. Discussion started: 13 December 2019

continental crustal thinning from north to south related to the increase of extension with increasing distance from the rotation pole of the anti-clockwise rotation of the Corsica-Sardinia block. Further, (3) seafloor spreading and formation of oceanic crust was not initiated during the extension of the Ligurian Basin. Thus, we assume that the oceanic domain does not extend as far north as previously stated and that the transition from the continental domain and the real oceanic domain is situated south or south-west, however, nearby our seismic line.

Data availability. Seismic data are available on request from the first or second author and will be made available via the German marine data archive PANGAEA upon acceptance of the manuscript.

Competing interests. The authors declare that they have no conflict of interest.

Acknowledgements. This project is funded by Deutsche Forschungsgemeinschaft (DFG), grant number KO_2961/6-1. We thank captain and crew of RV Maria S. Merian cruise MSM71 for their support during the OBS work. We thank the MSM71 cruise participants for their effort. The LOBSTER project comprises the offshore component of the AlpArray seismic network (Hetényi et al., 2018) and is part of the German priority program SPP2017 4D-MB. Generic Mapping Tools (Wessel & Smith, 1998) were used to produce the figures.

References

Advokaat, E. L., van Hinsbergen, D. J. J., Maffione, M., Langereis, C. G., Vissers, R. L. M., Cherchi, A., Schroeder, R., Madani, H. and Columbu, S.: Eocene rotation of Sardinia, and the paleogeography of the western Mediterranean region, Earth Planet. Sci. Lett., 401, 183–195, doi:10.1016/j.epsl.2014.06.012, 2014.

Bayer, R., Le Mouel, J. L. and Le Pichon, X.: Magnetic anomaly pattern in the western mediterranean, Earth Planet. Sci. Lett., 19(2), 168–176, doi:10.1016/0012-821X(73)90111-8, 1973.

Béthoux, N., Tric, E., Chery, J. and Beslier, M.-O.: Why is the Ligurian Basin (Mediterranean Sea) seismogenic? Thermomechanical modeling of a reactivated passive margin: MODELING OF THE LIGURIAN BASIN, Tectonics, 27(5), doi:10.1029/2007TC002232, 2008.

Bonatti, E., Seyler, M., Channell, J., Giraudeau, J. and Mascle, G., Eds.: Peridotites drilled from the Tyrrhenian Sea, ODP Leg 107, Ocean Drilling Program 107, 1990.

Bullock, A. and Minshull, T.: From continental extension to seafloor spreading: Crustal structure of the Goban Spur rifted margin, southwest of the UK, Geophys. J. Int., 163, 527–546, doi: 10.1111/j.1365-246X.2005.02726.x, 2005.

Burrus, J.: Contribution to a geodynamic synthesis of the Provencal Basin (NorthWestern Mediterranean), Mar. Geol., 55(3–4), 247–269, https://doi.org/10.1016/0025-3227(84)90071-9, 1984.

https://doi.org/10.5194/se-2019-187
Preprint. Discussion started: 13 December 2019

Carlson, R. L. and Miller, D. J.: Mantle wedge water contents estimated from seismic velocities in partially serpentinized peridotites: MANTLE WEDGE WATER CONTENTS, Geophys. Res. Lett., 30(5), doi:10.1029/2002GL016600, 2003.

Cella, F., Fedi, M., Florio, G., Paoletti, V. and Rapolla, A.: A review of the gravity and magnetic studies in the Tyrrhenian Basin and its volcanic districts, 23, 2008.

Chamot-Rooke, N., Jestin, F. and Gaulier, J.-M.: Constraints on Moho Depth and Crustal Thickness in the Liguro-Proven??al Basin from a 3d Gravity Inversion : Geodynamic Implications, Rev. Inst. FRANCAIS Pet., 52, 557–583, doi:10.2516/ogst:1997060, 1997.

Christensen, N. I. and Mooney, W. D.: Seismic velocity structure and composition of the continental crust: A global view, J. Geophys. Res. Solid Earth, 100(B6), 9761–9788, doi:10.1029/95JB00259, 1995.

Christeson, G. L., Goff, J. A. and Reece, R. S.: Synthesis of Oceanic Crustal Structure From Two-Dimensional Seismic Profiles, Rev. Geophys., 57(2), 504–529, doi:10.1029/2019RG000641, 2019.

Contrucci, I., Nercessian, A., Béthoux, N., Mauffret, A. and Pascal, G.: A Ligurian (Western Mediterranean Sea) geophysical transect revisited, Geophys. J. Int., 74–97, 2001.

Decarlis, A., Beltrando, M., Manatschal, G., Ferrando, S. and Carosi, R.: Architecture of the Distal Piedmont-Ligurian Rifted Margin in NW Italy: Hints for a Flip of the Rift System Polarity, Tectonics, 36(11), 2388–2406, doi:10.1002/2017TC004561, 2017.

Dercourt, J., Zonenshain, L. P., Ricou, L.-E., Kazmin, V. G., Le Pichon, X., Knipper, A. L., Grandjacquet, C., Sbortshikov, I. M., Geyssant, J., Lepvrier, C., Pechersky, D. H., Boulin, J., Sibuet, J.-C., Savostin, L. A., Sorokhtin, O., Westphal, M., Bazhenov, M. L., Lauer, J. P. and Biju-Duval, B.: Geological evolution of the tethys belt from the atlantic to the pamirs since the LIAS, Tectonophysics, 123(1–4), 241–315, doi:10.1016/0040-1951(86)90199-X, 1986.

Dessa, J.-X., Simon, S., Lelievre, M., Beslier, M.-O., Deschamps, A., Bethoux, N., Solarino, S., Sage, F., Eva, E., Ferretti, G., Bellier, O. and Eva, C.: The GROSMarin experiment: three dimensional crustal structure of the North Ligurian margin from refraction tomography and preliminary analysis of microseismic measurements, Bull. Soc. Geol. Fr., 182(4), 305–321, doi:10.2113/gssgfbull.182.4.305, 2011.

Doglioni, C., Gueguen, E., Sàbat, F. and Fernandez, M.: The Western Mediterranean extensional basins and the Alpine orogen, Terra Nova, 9(3), 109–112, doi:10.1046/j.1365-3121.1997.d01-18.x, 1997.

Faccenna, C., Mattei, M., Funiciello, R. and Jolivet, L.: Styles of back-arc extension in the Central Mediterranean, Terra Nova, 9(3), 126–130, doi:10.1046/j.1365-3121.1997.d01-12.x, 1997.

Faccenna, C., Funiciello, F., Giardini, D. and Lucente, P.: Episodic back-arc extension during restricted mantle convection in the Central Mediterranean, Earth Planet. Sci. Lett., 187(1–2), 105–116, doi:10.1016/S0012-821X(01)00280-1, 2001.

Fernàndez, M., Foucher, J. P. and Jurado, M. J.: Evidence for the multi-stage formation of the south-western Valencia Trough, Mar. Pet. Geol., 12(1), 101–109, doi:10.1016/0264-8172(95)90390-6, 1995.

https://doi.org/10.5194/se-2019-187
Preprint. Discussion started: 13 December 2019

Finetti, I. R., Boccaletti, M., Bonini, M., Ben, A., Pipan, M., Prizzon, A. and Sani, F.: Lithospheric Tectono-Stratigraphic Setting of the Ligurian Sea–Northern Apennines–Adriatic Foreland from Integrated CROP Seismic Data, in Deep Seismic Exploration of the Central Mediterranean and Italy, CROP PROJECT, pp. 119–158., 2005.

Fujie, G., Kasahara, J., Murase, K., Mochizuki, K. and Kaneda, Y.: Interactive analysis tools for the wide-angle seismic data for crustal structure study (Technical Report), Explor. Geophys. - EXPLOR GEOPHYS, 39, doi:10.1071/EG08006, 2008.

Gailler, A., Klingelhoefer, F., Olivet, J.-L. and Aslanian, D.: Crustal structure of a young margin pair: New results across the Liguro–Provencal Basin from wide-angle seismic tomography, Earth Planet. Sci. Lett., 286(1–2), 333–345, doi:10.1016/j.epsl.2009.07.001, 2009.

Gardner, G. H. F., Gardner, L. W. and Gregory, A. R.: FORMATION VELOCITY AND DENSITY—THE DIAGNOSTIC BASICS FOR STRATIGRAPHIC TRAPS, GEOPHYSICS, 39(6), 770–780, doi:10.1190/1.1440465, 1974.

Grevemeyer, I., Ranero, C. R. and Ivandic, M.: Structure of oceanic crust and serpentinization at subduction trenches, Geosphere, 14(2), 395–418, doi:10.1130/GES01537.1, 2018.

Gueguen, E., Doglioni, C. and Fernandez, M.: On the post-25 Ma geodynamic evolution of the western Mediterranean, Tectonophysics, 298(1–3), 259–269, doi:10.1016/S0040-1951(98)00189-9, 1998.

Guerin, G., Rivet, D., Deschamps, A., Larroque, C., Mordret, A., Dessa, J.-X. and Martin, X.: High resolution ambient noise tomography of the South-Western Alps and the Ligurian margin, Geophys. J. Int., doi:10.1093/gji/ggz477, 2019.

Handy, M. R., M. Schmid, S., Bousquet, R., Kissling, E. and Bernoulli, D.: Reconciling plate-tectonic reconstructions of Alpine Tethys with the geological–geophysical record of spreading and subduction in the Alps, Earth-Sci. Rev., 102(3–4), 121–158, doi:10.1016/j.earscirev.2010.06.002, 2010.

Hetényi, G., Molinari, I., Clinton, J., Bokelmann, G., Bondár, I., Crawford, W. C., Dessa, J.-X., Doubre, C., Friederich, W., Fuchs, F., Giardini, D., Gráczer, Z., Handy, M. R., Herak, M., Jia, Y., Kissling, E., Kopp, H., Korn, M., Margheriti, L., Meier, T., Mucciarelli, M., Paul, A., Pesaresi, D., Piromallo, C., Plenefisch, T., Plomerová, J., Ritter, J., Rümpker, G., Šipka, V., Spallarossa, D., Thomas, C., Tilmann, F., Wassermann, J., Weber, M., Wéber, Z., Wesztergom, V., Živčić, M., Abreu, R., Allegretti, I., Apoloner, M.-T., Aubert, C., Besançon, S., Bès de Berc, M., Brunel, D., Capello, M., Čarman, M., Cavaliere, A., Chèze, J., Chiarabba, C., Cougoulat, G., Cristiano, L., Czifra, T., D'Alema, E., Danesi, S., Daniel, R., Dannowski, A., Dasović, I., Deschamps, A., Egdorf, S., Fiket, T., Fischer, K., Funke, S., Govoni, A., Gröschl, G., Heimers, S., Heit, B., Herak, D., Huber, J., Jarić, D., Jedlička, P., Jund, H., Klingen, S., Klotz, B., Kolínský, P., Kotek, J., Kühne, L., Kuk, K., Lange, D., Loos, J., Lovati, S., Malengros, D., Maron, C., Martin, X., Massa, M., Mazzarini, F., Métral, L., Moretti, M., Munzarová, H., Nardi, A., Pahor, J., Péquegnat, C., Petersen, F., Piccinini, D., Pondrelli, S., Prevolnik, S., Racine, R., Régnier, M., Reiss, M., Salimbeni, S., et al.: The AlpArray Seismic Network: A Large-Scale European Experiment to Image the Alpine Orogen, Surv. Geophys., 39(5), 1009–1033, doi:10.1007/s10712-018-9472-4, 2018.

Jolivet, L. and Faccenna, C.: Mediterranean extension and the Africa-Eurasia collision, Tectonics, 19(6), 1095–1106, doi:10.1029/2000TC900018, 2000.

https://doi.org/10.5194/se-2019-187
Preprint. Discussion started: 13 December 2019

Jolivet, L., Gorini, C., Smit, J. and Leroy, S.: Continental breakup and the dynamics of rifting in back-arc basins: The Gulf of Lion margin: Backarc rift and lower crust extraction, Tectonics, 34(4), 662–679, doi:10.1002/2014TC003570, 2015.

Kopp, H., Lange, D., Thorwart, M., Paul, A., Dannowski, A., Petersen, F., Aubert, C., Beeck, F., Beniest, A., Besançon, S., Brotzer, A., Caielli, G., Crawford, W., Deen, M., Lehmann, C., Marquardt, K., Neckel, M., Papanagnou, L., Schramm, B., Schröder, P., Steffen, K.-P., Wolf, F., Xia, Y.: RV MARIA S. MERIAN Fahrtbericht / Cruise Report MSM71 LOBSTER: Ligurian Ocean Bottom Seismology and Tectonics Research, Las Palmas (Spain) – Heraklion (Greece) 07.02.-27.02.2018. GEOMAR Report, N. Ser. 041 . GEOMAR Helmholtz-Zentrum für Ozeanforschung Kiel, Kiel, Germany, 47 pp, doi: 10.3289/GEOMAR_REP_NS_41_2018 , 2018.

Korenaga, J., Holbrook, W. S., Kent, G. M., Kelemen, P. B., Detrick, R. S., Larsen, H.-C., Hopper, J. R. and Dahl-Jensen, T.: Crustal structure of the southeast Greenland margin from joint refraction and reflection seismic tomography, J. Geophys. Res. Solid Earth, 105(B9), 21591–21614, doi:10.1029/2000JB900188, 2000.

Korenaga, J., Holbrook, W. S., Detrick, R. S. and Kelemen, P. B.: Gravity anomalies and crustal structure at the southeast Greenland margin, J. Geophys. Res. Solid Earth, 106(B5), 8853–8870, doi:10.1029/2000JB900416, 2001.

Le Douaran, S., Burrus, J. and Avedik, F.: Deep structure of the north-western Mediterranean Basin: Results of a two-ship seismic survey, Mar. Geol., 55(3–4), 325–345, doi:10.1016/0025-3227(84)90075-6, 1984.

Makris, J., Egloff, F., Nicolich, R. and Rihm, R.: Crustal structure from the Ligurian Sea to the Northern Apennines — a wide angle seismic transect, Tectonophysics, 301(3–4), 305–319, doi:10.1016/S0040-1951(98)00225-X, 1999.

Mauffret, A., Pascal, G., Maillard, A. and Gorini, C.: Tectonics and deep structure of the north-western Mediterranean Basin, Mar. Pet. Geol., 12(6), 645–666, doi:10.1016/0264-8172(95)98090-R, 1995.

Minshull, T. A., Dean, S. M. and Whitmarsh, R. B.: The peridotite ridge province in the southern Iberia Abyssal Plain: Seismic constraints revisited, J. Geophys. Res. Solid Earth, 119(3), 1580–1598, doi:10.1002/2014JB011011, 2014.

Moeller, S., Grevemeyer, I., Ranero, C. R., Berndt, C., Klaeschen, D., Sallares, V., Zitellini, N. and de Franco, R.: Early-stage rifting of the northern Tyrrhenian Sea Basin: Results from a combined wide-angle and multichannel seismic study: Rifting Tyrrhenian, Geochem. Geophys. Geosystems, 14(8), 3032–3052, doi:10.1002/ggge.20180, 2013.

Montigny, R., Edel, J. B. and Thuizat, R.: Oligo-Miocene rotation of Sardinia: KAr ages and paleomagnetic data of Tertiary volcanics, Earth Planet. Sci. Lett., 54(2), 261–271, doi:10.1016/0012-821X(81)90009-1, 1981.

Nagel, T. J. and Buck, W. R.: Symmetric alternative to asymmetric rifting models, Geology, 32(11), 937, doi:10.1130/G20785.1, 2004.

Pascal, G. P., Mauffret, A. and Patriat, P.: The ocean-continent boundary in the Gulf of Lion from analysis of expanding spread profiles and gravity modelling, Geophys. J. Int., 113(3), 701–726, doi:10.1111/j.1365-246X.1993.tb04662.x, 1993.

Pérez-Gussinyé, M.: A tectonic model for hyperextension at magma-poor rifted margins: an example from the West Iberia–Newfoundland conjugate margins, Geol. Soc. Lond. Spec. Publ., 369(1), 403–427, doi:10.1144/SP369.19, 2013.

https://doi.org/10.5194/se-2019-187
Preprint. Discussion started: 13 December 2019

Prada, M., Sallares, V., Ranero, C. R., Vendrell, M. G., Grevemeyer, I., Zitellini, N. and de Franco, R.: Seismic structure of the Central Tyrrhenian basin: Geophysical constraints on the nature of the main crustal domains: CRUSTAL AFFINITY OF THE TYRRHENIAN BASIN, J. Geophys. Res. Solid Earth, 119(1), 52–70, doi:10.1002/2013JB010527, 2014.

Prada, M., Ranero, C. R., Sallarès, V., Zitellini, N. and Grevemeyer, I.: Mantle exhumation and sequence of magmatic events in the Magnaghi–Vavilov Basin (Central Tyrrhenian, Italy): New constraints from geological and geophysical observations, Tectonophysics, 689, 133–142, doi:10.1016/j.tecto.2016.01.041, 2016.

Réhault, J.-P. and Bethoux, N.: Earthquake relocation in the Ligurian Sea (western Mediterranean): Geological interpretation, Mar. Geol., 55(3), 429–445, doi:10.1016/0025-3227(84)90080-X, 1984.

Réhault, J.-P., Boillot, G. and Mauffret, A.: The Western Mediterranean Basin geological evolution, Mar. Geol., 55(3), 447–477, doi:10.1016/0025-3227(84)90081-1, 1984.

Réhault, J.-P., Honthaas, C., Guennoc, P., Bellon, H., Ruffet, G., Cotten, J., Sosson, M. and Maury, R. C.: Offshore Oligo-Miocene volcanic fields within the Corsica-Liguria Basin: Magmatic diversity and slab evolution in the western Mediterranean Sea, J. Geodyn., 58, 73–95, doi:10.1016/j.jog.2012.02.003, 2012.

Roca, E. and Desegaulx, P.: Analysis of the geological evolution and vertical movements in the València Trough area, western Mediterranean, Mar. Pet. Geol., 9(2), 167–185, doi:10.1016/0264-8172(92)90089-W, 1992.

Rollet, N., Déverchère, J., Beslier, M.-O., Guennoc, P., Réhault, J.-P., Sosson, M. and Truffert, C.: Back arc extension, tectonic inheritance, and volcanism in the Ligurian Sea, Western Mediterranean: LIGURIAN SEA BACK ARC STRUCTURE AND EVOLUTION, Tectonics, 21(3), 6-1-6–23, doi:10.1029/2001TC900027, 2002.

Rosenbaum, G., Lister, G. and Duboz, C.: Reconstruction of the tectonic evolution of the Western Mediterranean since the Oligocene, J. Virtual Explor., 8, 107–130, doi:10.3809/jvirtex.2002.00053, 2002.

Sandwell, D. T., Müller, R. D., Smith, W. H. F., Garcia, E. and Francis, R.: New global marine gravity model from CryoSat-2 and Jason-1 reveals buried tectonic structure, Science, 346(6205), 65, doi:10.1126/science.1258213, 2014.

Speranza, F., Villa, I. M., Sagnotti, L., Florindo, F., Cosentino, D., Cipollari, P. and Mattei, M.: Age of the Corsica–Sardinia rotation and Liguro–Provençal Basin spreading: new paleomagnetic and Ar/Ar evidence, Tectonophysics, 347(4), 231–251, doi:10.1016/S0040-1951(02)00031-8, 2002.

Talwani, M., Worzel, J. L. and Landisman, M.: Rapid gravity computations for two-dimensional bodies with application to the Mendocino submarine fracture zone, J. Geophys. Res. 1896-1977, 64(1), 49–59, doi:10.1029/JZ064i001p00049, 1959.

Vigliotti, L. and Langenheim, V. E.: When did Sardinia stop rotating? New palaeomagnetic results, Terra Nova, 7(4), 424–435, doi:10.1111/j.1365-3121.1995.tb00538.x, 1995.

Wessel, P., & Smith, W. H. F.: New improved version of the generic mapping tools released. Eos, Transactions American Geophysical Union, 79(47), 579. https://doi.org/10.1029/98EO00426, 1998.

White, R. S., McKenzie, D. and O'Nions, R. K.: Oceanic crustal thickness from seismic measurements and rare earth element inversions, J. Geophys. Res., 97(B13), 19683, doi:10.1029/92JB01749, 1992.

https://doi.org/10.5194/se-2019-187
Preprint. Discussion started: 13 December 2019

Zelt, C. A.: Modelling strategies and model assessment for wide-angle seismic traveltime data, Geophys. J. Int., 139(1), 183–204, doi:10.1046/j.1365-246X.1999.00934.x, 1999.

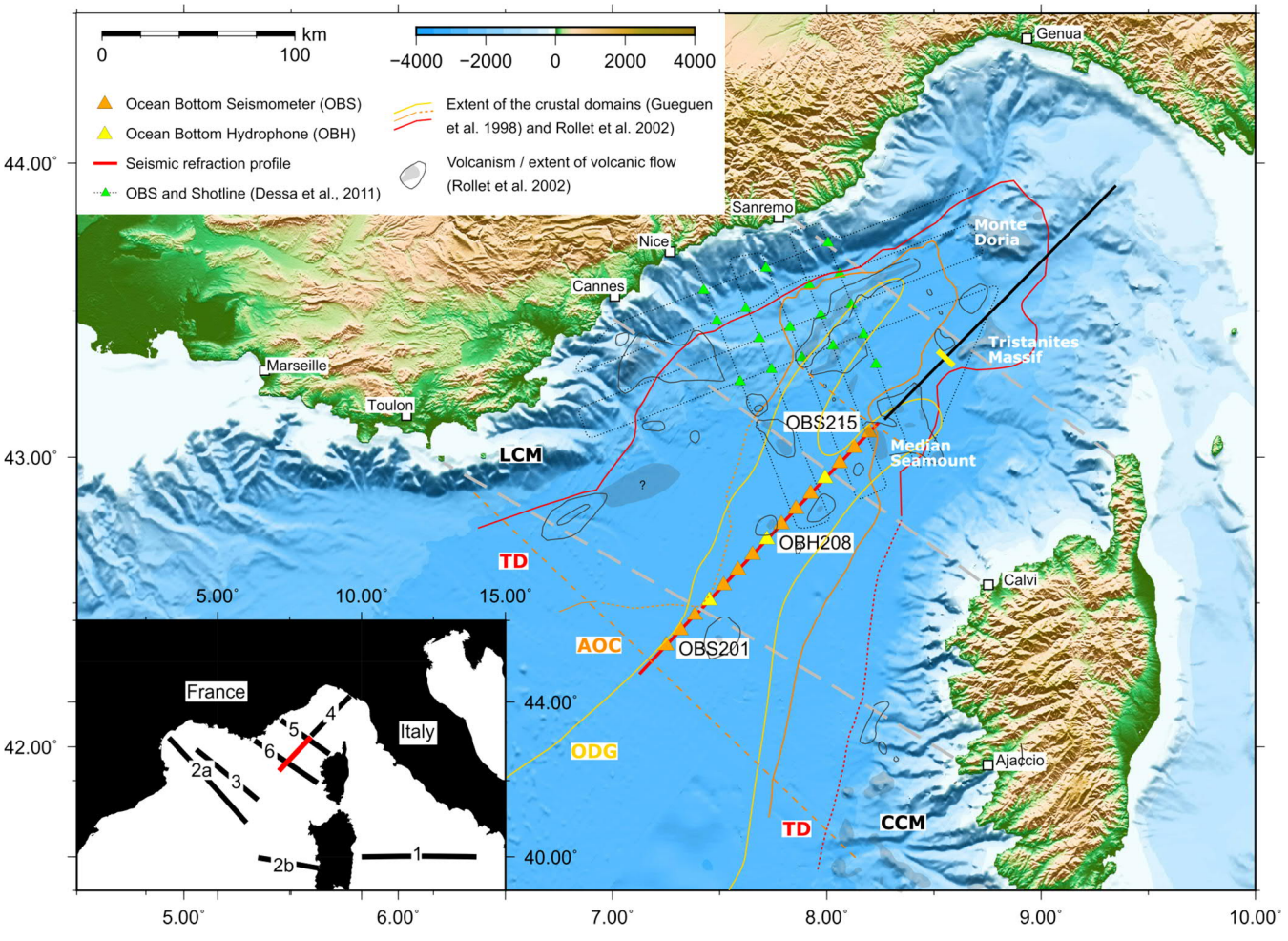

Figure 1: Map of the study area with the seismic refraction line (thick red line) and OBH/OBS locations. Thin black lines and grey shaded areas mark volcanic extrusion after Rollet et al. (2002). The different crustal domains (Rollet et al., 2002) are marked by thin orange and red lines and labled with: AOC - atypical oceanic crust, CCM - Corsica continental margin, LCM - Ligurian continental margin, TD - transitional domain. Thin yellow line marks the oceanic domain (ODG) after Gueguen et al. (1998). Red dashed lines show proposed fracture zones (Rollet et al., 2002). Green triangles and dotted lines are the OBS locations and shot profiles of Dessa et al. (2011). The black and white inset in the lower left corner show previous seismic refraction and reflection lines: 1 - Prada et al. (2014), 2a/2b - Gailler et al. (2009), 3 - Jolivet et al. (2015), 4 - Makris et al. (1999), 5 - Contrucci et al. (2001), 6 - MA24 from Rollet et al. (2002).

https://doi.org/10.5194/se-2019-187
Preprint. Discussion started: 13 December 2019

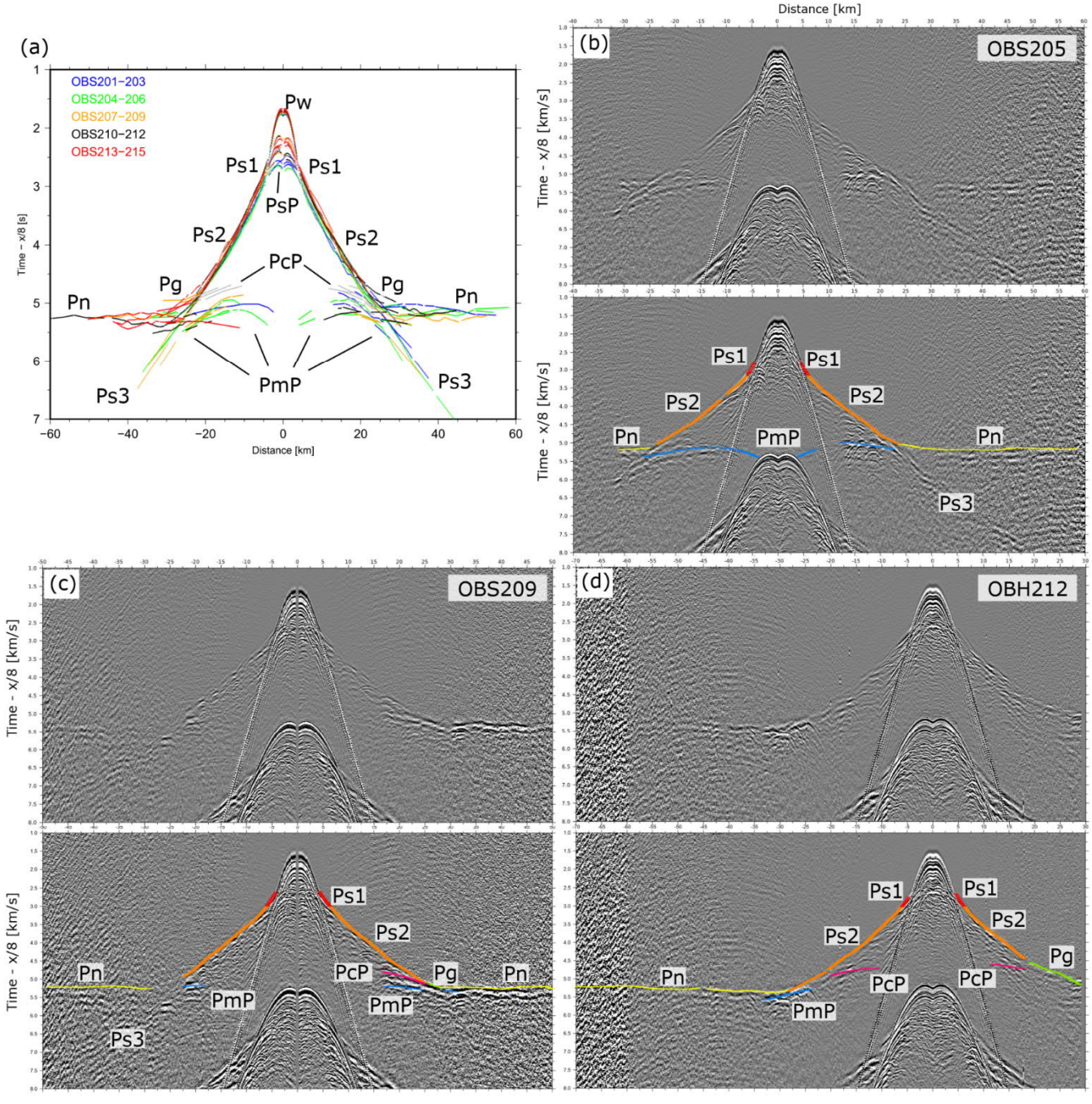

Figure 2: (a) Stacked travel time picks of all 15 stations showing very similar arrivals suggesting an almost 1D structure along the profile. (b) Record section of station OBS205 (time reduced with a velocity of 8 km/s). The lower panel shows the calculated travel time picks from the final velocity model superimposed on the seismic data. (c) Record section and calculated travel times of station OBS209 (d) Record section and calculated travel times of station OBH212.

https://doi.org/10.5194/se-2019-187
Preprint. Discussion started: 13 December 2019

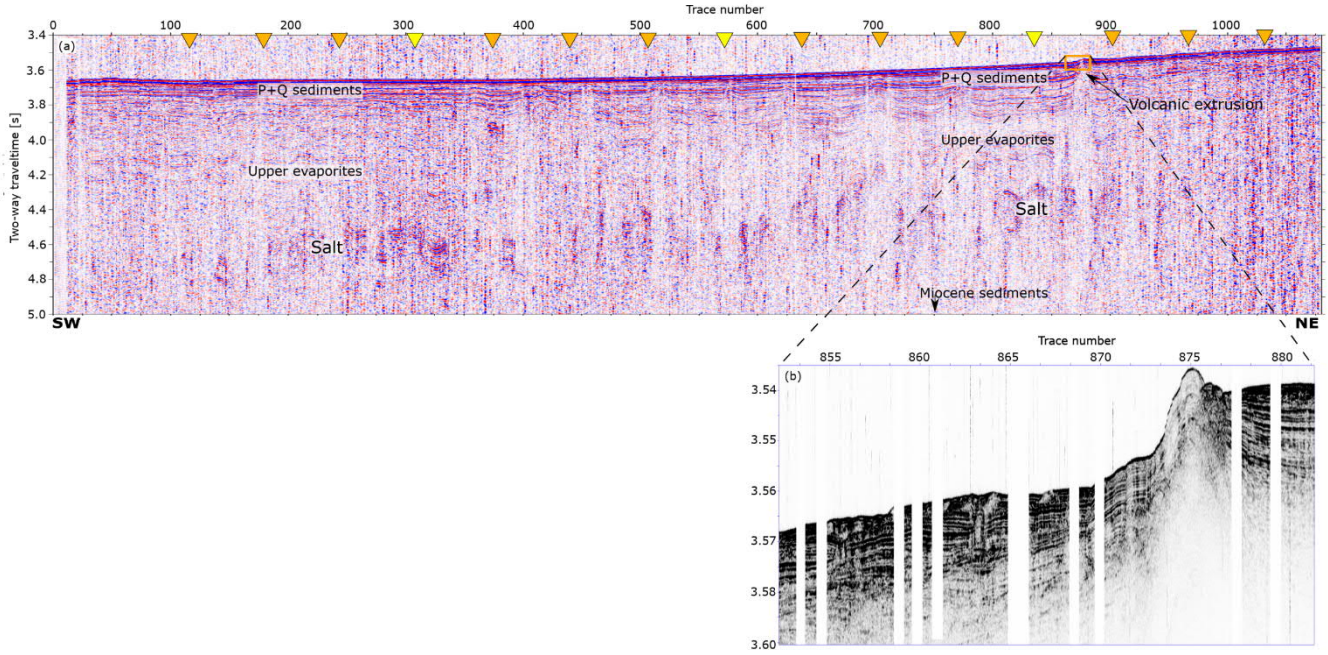

530

Figure 3: Multi-channel seismic data (MCS data) simultaneously shot with the refraction seismic line. The orange/yellow triangles mark the OBS/OBH positions along the profile. Parasound data from the orange box shown in the lower panel.

https://doi.org/10.5194/se-2019-187
Preprint. Discussion started: 13 December 2019

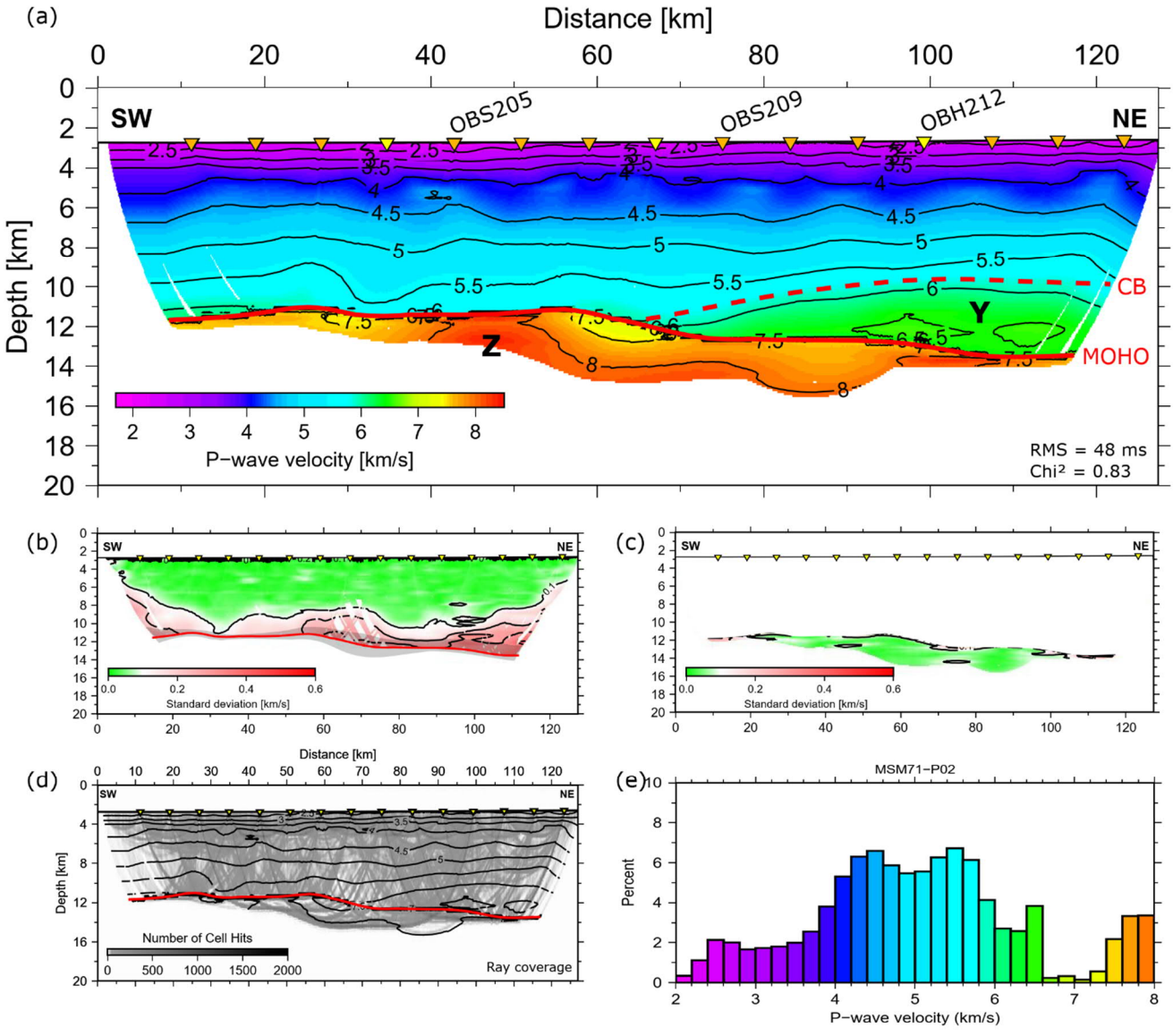

535 **Figure 4: (a) Final velocity model based on the averaged velocities from the plausible starting models. The red dashed line marks the crystalline basement (CB) and the solid red line marks the crust-mantle boundary (Moho); (b) Standard deviation for 17 inverted velocity models, covering the crustal part down to the Moho; (c) Standard deviation for 12 inverted velocity models, covering the upper mantle up to the Moho; (d) Ray coverage for the final average velocity model; (e) Histogram with the velocity distribution of the final average velocity model.**

https://doi.org/10.5194/se-2019-187
Preprint. Discussion started: 13 December 2019

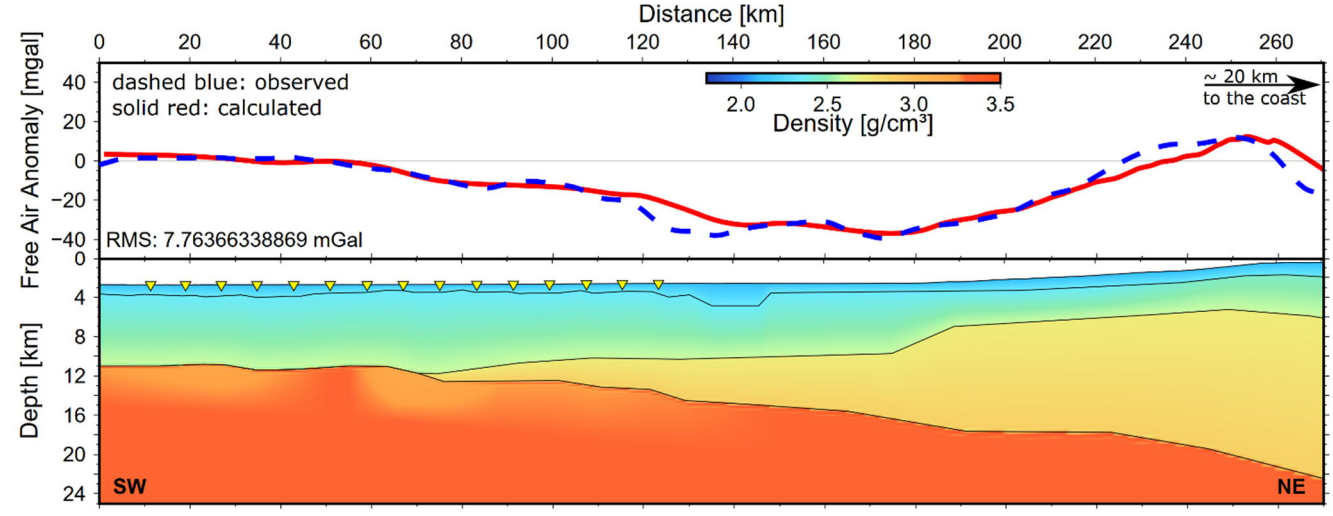

Figure 5: Figure 5 – Density model (lower panel) converted from seismic velocities to densities for the SW part covered by seismic stations. The profile was extended towards the NE using the marine part of the seismic refraction line of Makris et al. (1999). The upper panel shows the data fit between the observed free-air anomaly data (dashed blue) and the model response (solid red line).